NASA TN D-52

TN-26
195450
22p

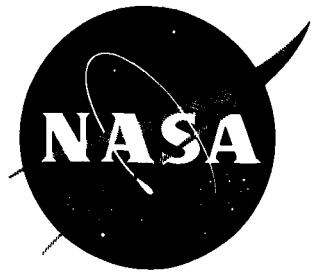

TECHNICAL NOTE
D-52

THE RATE OF FATIGUE-CRACK PROPAGATION FOR TWO ALUMINUM ALLOYS UNDER COMPLETELY REVERSED LOADING

By Walter Illg and Arthur J. McEvily, Jr.

Langley Research Center
Langley Field, Va.

NATIONAL AERONAUTICS AND SPACE ADMINISTRATION

WASHINGTON

October 1959

(NASA-TN-D-52) THE RATE OF FATIGUE-CRACK PROPAGATION FOR TWO ALUMINUM ALLOYS UNDER COMPLETELY REVERSED LOADING (NASA) 22 p

N89-70477

Unclas
00/26 0195450

1Y

NATIONAL AERONAUTICS AND SPACE ADMINISTRATION

TECHNICAL NOTE D-52

THE RATE OF FATIGUE-CRACK PROPAGATION FOR TWO ALUMINUM ALLOYS UNDER COMPLETELY REVERSED LOADING

By Walter Illg and Arthur J. McEvily, Jr.

SUMMARY

A series of fatigue-crack propagation tests of two aluminum-alloy sheet specimens has been conducted under completely reversed loading at various stress levels up to 30 ksi. Differences between effects of the compression and tension parts of the cycles are discussed. Semiempirical equations are developed which permit calculation of crack growth. Results are compared with those from similar tests made at a minimum stress of 1 ksi. In both types of loading, the governing parameter was found to be related to the local stress at the crack tip.

INTRODUCTION

Knowledge of the significant parameters affecting the rate of propagation of fatigue cracks is useful in the application of fail-safe design. A previous paper, reference 1, presented the results of fatigue-crack propagation tests performed on sheet specimens of 2024-T3 and 7075-T6 aluminum alloys. These specimens were subjected to repeated tension loading with a minimum stress of 1 ksi and a maximum stress which varied from test to test from 3 to 50 ksi. It was found in reference 1 that the crack propagation rates depended explicitly on the product of stress-concentration factor and net stress and were influenced by specimen width only insofar as it entered into the determination of that product. Semiempirical expressions, based on a stress-concentration factor at the tip of the crack, were developed which compared favorably with experimental results.

The purpose of the present paper is to extend this work to completely reversed loading. The evaluation presented in reference 1 indicated that the rate of crack propagation was dependent solely upon the product of the stress-concentration factor and net stress irrespective of specimen width; therefore, subsequent investigations need employ but one convenient width of specimen rather than several widths. Accordingly, five specimens of 2024-T3 aluminum alloy and three specimens of 7075-T6 aluminum alloy,

12 inches wide, were tested to determine the rate of fatigue-crack propagation under maximum net stresses varying from test to test from 6 to 30 ksi. Separate specimens of each material were tested in order to find the fatigue limit of a specimen containing a fatigue crack, and other specimens were used to determine material properties.

The results of the present tests are compared with those from reference 1 which involved only tension loading. The relative importance in fatigue-crack propagation of tension and compression are discussed.

L 3 2 8

SYMBOLS

A_1, A_2, A_3	constants in fatigue-crack-rate expression
a	one-half of major axis of ellipse, in.
C	constant of integration, cycles
c	half-width of sheet, in.
K_E	theoretical stress-concentration factor for ellipse
K_H	theoretical stress-concentration factor for circular hole
K_N	theoretical stress-concentration factor modified for size effect
K_T	theoretical stress-concentration factor
N	number of cycles
R	ratio of minimum stress to maximum stress
r	rate of fatigue-crack propagation, in./cycle
S_f	fatigue limit (or stress at 10^8 cycles), ksi
S_{net}	maximum load divided by remaining net sectional area, ksi
S_o	maximum load divided by initial net sectional area, ksi

x one-half of total length of central symmetrical crack, in.

α stress-dependent proportionality constant, in.$^{-1/2}$/cycle

ρ radius of curvature, in.

ρ' Neuber material constant, in.

ρ_e effective radius of curvature at tip of fatigue crack, in.

SPECIMENS AND TESTS

All specimens used in this investigation for the study of fatigue-crack propagation rate were cut from a single sheet of each of the aluminum alloys 2024-T3 and 7075-T6 of 0.081-inch nominal thickness. Figure 1 shows the specimen configuration. The specimens were 12 inches wide and contained a 1/16-inch-diameter hole at the midpoint which was notched on each side to a depth of 1/32 inch. The radius at the root of the notch was 0.005 inch and this configuration had a theoretical stress-concentration factor of 7.9. The notch-cutting procedure is described in reference 1.

The surface of the specimen was polished as described in reference 1 and fine longitudinal lines were scribed with a razor blade to facilitate measurement of crack growth. Since the present tests were run under completely reversed loading, two guide plates were used to prevent buckling in compression. One of the guide plates contained a $\frac{1}{2}$ - by 5-inch cutout to allow visual observation of the region of the crack.

The tests in which the maximum stresses were greater than 10 ksi were performed in a ±120,000-pound-capacity hydraulic jack which cycled automatically at speeds of approximately 9 to 13 cpm (ref. 2). One of these tests was duplicated at 1,200 cpm in a ±100,000-pound-capacity hydraulic fatigue machine to check speed effect. All other tests were performed in subresonant-type fatigue machines which operated at 1,800 cpm and had a capacity of ±20,000 pounds (ref. 3).

The specimens were illuminated with a stroboscopic light and crack progress was observed continuously through a 30-power microscope. The numbers of cycles required to initiate a crack and to cause the crack to reach each scribed line were recorded.

The maximum and minimum loads remained constant throughout each test, and the tests were conducted up to values of S_o of 30 ksi with

one specimen tested at each of several levels. The tests were terminated when the rate of crack propagation became too rapid for accurate observation or when the cracks grew beyond the cutout region provided for visual observation.

Two special types of tests were performed for each material on 2-inch-wide specimens in order to determine the stress at which a fatigue crack will not propagate under completely reversed loading (R = -1). In one type of test, the crack was initiated in a 0.005-inch-radius notch ($K_T = 7.4$) at $S_o = 10$ ksi and was propagated to a total length of 1/2 inch at 7 ksi. The stress was progressively reduced until a level was found at which the crack did not propagate in 10^8 cycles. In the other type of test, the crack was initiated in a 0.001-inch-radius notch ($K_T = 16$) at a value of $K_N S_{net}$ of 26 ksi. The latter type of test was made to determine whether the cracks would propagate, and no data on the rate of propagation were obtained.

L 3 2 8

In addition, standard tensile tests were performed to determine the 0.2-percent-offset yield stress, the ultimate strength, the total elongation, and the Young's modulus for each of the two materials.

RESULTS AND DISCUSSION

Mechanical Properties

The mechanical properties of the two aluminum alloys as determined from the average of four standard tensile tests for each material are as follows:

	2024-T3	7075-T6
Yield stress (0.2-percent offset), ksi	53.1	74.5
Ultimate strength, ksi	71.2	81.1
Total elongation (2-inch gage length), percent	19.3	12.6
Young's modulus, ksi	11.00×10^3	10.61×10^3

Fatigue-Crack Propagation

The fatigue-crack propagation results are summarized in table I which gives the number of cycles required to extend a crack from an initial total length of 0.2 inch to specified lengths. These crack lengths are plotted in figure 2 against number of cycles. The rate of

crack propagation was obtained graphically by measuring the slopes of the curves in figure 2 at various crack lengths. The rates of fatigue-crack propagation have been plotted in figure 3 against the parameter $K_N S_{net}$, which was shown in reference 1 to be the parameter governing the rate of fatigue-crack propagation. The stress-concentration factor K_N was computed by the method outlined in the appendix. The values of ρ' necessary for these computations were taken from reference 1 and are 0.003 inch for 2024-T3 aluminum alloy and 0.002 inch for 7075-T6 aluminum alloy.

Examination of figure 3 reveals that the fatigue-crack propagation rates for each material are essentially single-valued functions of the parameter $K_N S_{net}$. For purposes of comparison the previously published curve (ref. 1) for $R \approx 0$ is also shown in this figure. It is apparent that over the lower range for the 2024-T3 specimen and over the entire range for the 7075-T6 specimen, the rate of fatigue-crack propagation at $R = -1$ is essentially the same as at $R \approx 0$.

This result can be explained in the following manner. In the region where the rates for $R = -1$ and $R \approx 0$ are about the same, the compression part of the $R = -1$ cycle must have little effect on the rate of crack propagation. This would be the case if the crack surfaces were brought into contact during the compression part of the cycle so that the effective net sectional area would be increased and the stress concentration at the tip of the crack would be eliminated. The primary source of damage in such a case is the tension part of the cycle. However, for values of $K_N S_{net}$ in excess of 100 ksi, the rate of fatigue-crack propagation is higher at $R = -1$ than at $R \approx 0$ for 2024-T3 aluminum alloy. The compression part of the cycle must have an effect in this material, and in line with the preceding explanation the compressive cycle should have an effect only if the crack did not close completely. This may indeed be the case for the 2024-T3 material at high $K_N S_{net}$ levels. At such levels, the material at the base of the notch would be subjected to large plastic deformation during the tension part of the cycle because of the relatively low yield strength of 2024-T3 aluminum alloy. Then the crack surfaces could not be readily closed up in the following compression part of the cycle. In such a case, the effective net sectional area would not be increased and the stress-concentration effect would remain. Thus the material at the tip of the crack would be subjected to a more drastic stress history than it would if the crack were to close completely. Evidence that this is the proper explanation is given in figure 4 where it is seen that fatigue cracks in specimens tested at a high stress level are wider in 2024-T3 than in 7075-T6 specimens. In addition, localized plastic deformation at the tip of the crack was more apparent in the 2024-T3 specimens than in the 7075-T6 specimens.

The results of the tests on 2024-T3 aluminum alloy at $S_o = 20$ ksi at the two cycling speeds, 13 and 1,200 cpm, indicate a slight speed effect since the fatigue-crack propagation rates at 1,200 cpm are generally somewhat smaller than those at 13 cpm (fig. 3). Inasmuch as the check involved only two specimens, the results are by no means conclusive - especially in view of results of speed-effect tests performed at $R \approx 0$ (ref. 1) wherein no consistent speed effects were found.

Minimum Value of $K_N S_{net}$ Required to Propagate a Fatigue Crack

Crack propagation was found to cease in the stepped-stress tests when the value of $K_N S_{net}$ had been reduced to 22 ksi for 2024-T3 aluminum alloy and 20.5 ksi for 7075-T6 aluminum alloy. These appear to be the minimum stresses which will result in crack propagation when the stresses are continuously reduced and are very nearly equal to the fatigue limit of an unnotched specimen (20 ksi for each material, ref. 3). In the constant-load tests which utilized the 0.001-inch notch as the initial stress raiser, it was found that the cracks did propagate at $K_N S_{net} = 26$ ksi for each material. The fact that cracks propagated in these tests supports the belief that the decreasing load method indicates correctly the lowest stress at which cracks will propagate.

Since the minimum values of $K_N S_{net}$ for propagation at $R = -1$ are below the fatigue limit for unnotched specimens at $R \approx 0$ (approximately 30 ksi) and are close to the fatigue limit for unnotched specimens at $R = -1$, the compression part of the cycle has been of influence in these low-stress tests; it may be that at these low levels complete closure is not obtained.

Semiempirical Curves

A mathematical representation of the data in figure 3 would be useful for calculating the number of cycles required to lengthen a crack a specified amount. A form of the semiempirical expression developed in reference 1 was applied to fit the present data by using appropriate constants. The general form of this equation is

$$\log_{10} r = A_1 K_N S_{net} + A_2 + A_3 \frac{S_f}{K_N S_{net} - S_f} \qquad (1)$$

L 3 2 8

where S_f is the fatigue limit of the particular material for a given value of R, as obtained from tests of unnotched specimens. The expressions for the two aluminum alloys tested at $R = -1$ are taken as follows:

For 2024-T3

$$\log_{10} r = 0.00590K_N S_{net} - 5.20 - 2.94 \frac{20}{K_N S_{net} - 20} \tag{2}$$

and for 7075-T6

$$\log_{10} r = 0.00495K_N S_{net} - 5.37 - 2.60 \frac{20}{K_N S_{net} - 20} \tag{3}$$

Equation (3) represents a curve essentially identical with the single curve which fitted all the data for both materials at $R \approx 0$ (ref. 1). The equation for the fitted curve from reference 1 is

$$\log_{10} r = 0.00509K_N S_{net} - 5.472 - \frac{34}{K_N S_{net} - 34} \tag{4}$$

Equations (2), (3), and (4) are plotted in figure 3.

The smaller fatigue limit of 20 ksi at $R = -1$ requires the constants A_1, A_2, and A_3 to take on different values even though equations (3) and (4) represent nearly identical curves. Integration of equations (2) and (3) would require tedious numerical methods. Consequently, the simpler approximate method developed in reference 1 will be employed. This method utilizes a formula for crack growth proposed by Head (ref. 4):

$$r = \frac{dx}{dN} = 2\alpha x^{3/2} \tag{5}$$

where x is one-half the crack length and α is a constant for a given stress level and material. Integration of this expression (eq. (5)) yields

$$N = C - \frac{1}{\alpha\sqrt{x}} \tag{6}$$

where C is a constant of integration which may be evaluated from boundary conditions.

Values of α were found for a number of crack lengths for each stress level by equating the expression for the rate in equation (5) with that in either equation (2) or (3). These equations are good approximations of the actual rates of crack propagation as found by experiment. Since the greatest number of cycles occur at the shorter crack lengths, the values of α were weighted accordingly. Each value of α was multiplied by the reciprocal of the rate of crack propagation and the weighted average was then determined. The results of these calculations are presented in table II. These values for α were used in equation (6) to predict the number of cycles required to extend the fatigue cracks from an initial length of 0.2 inch to various final lengths for all the tests. The results are given in figure 2 as dashed lines. Although α varied considerably for the final 20 percent of life, the maximum ratio of predicted to actual life is less than 2:1. Therefore, the agreement between the number of cycles required to extend the 0.2-inch crack to specific lengths, calculated with the use of the semiempirical expression, are in acceptable agreement with the experimental results inasmuch as even more scatter is usually associated with fatigue test results.

L
3
2
8

CONCLUDING REMARKS

A series of crack propagation tests have been run in sheet specimens of 2024-T3 and 7075-T6 aluminum alloys under completely reversed loading $\left(R = \frac{\text{Minimum load}}{\text{Maximum load}} = -1\right)$ and the results compared with previous tests made at $R \approx 0$. As was the case for $R \approx 0$, the theoretical stress-concentration factor modified for size effect times the net-section stress ($K_N S_{net}$) was found to be a useful parameter for correlating the results of these tests. The rate of fatigue-crack propagation in 7075-T6 aluminum alloy was the same at both $R \approx 0$ and $R = -1$ over practically the entire range of stresses investigated. In 2024-T3 aluminum alloy, the rate was the same for both R values only at values of $K_N S_{net}$ between approximately 50 and 100 ksi; higher stresses resulted in higher rates at $R = -1$ than at $R \approx 0$. The close agreement found between $R \approx 0$ and $R = -1$ tests has been explained on the basis of crack closure during compression. Consequently, the main factor influencing fatigue-crack propagation in general is the tension part of the cycle.

The numbers of cycles required to extend a 0.2-inch crack to specific lengths, calculated with the use of a semiempirical expression, were in acceptable agreement with experimental results.

Langley Research Center,
National Aeronautics and Space Administration,
Langley Field, Va., July 6, 1959.

APPENDIX

METHOD FOR CALCULATION OF K_N

A brief description will be given of the method for determination of the stress-concentration factor corrected for size effect K_N.

In the present investigation the stress raiser is a central symmetrical crack and is considered to be an ellipse with major axis equal to the total length of the crack. The procedure for finding the stress-concentration factor for an ellipse involves first determining the factor for a circular hole K_H with diameter equal to the major axis of the ellipse from Howland's curve (fig. 5). The second step is to adjust this value to convert it into a factor for an elliptical hole, as follows:

$$K_E = 1 + (K_H - 1)\sqrt{\frac{a}{\rho}} \tag{A1}$$

where K_E is the stress-concentration factor for the ellipse, a is the semimajor axis of the ellipse, and ρ is the tip radius of the ellipse.

The last step is to correct K_E for size effect by using the Neuber formula:

$$K_N = 1 + \frac{K_E - 1}{1 + \sqrt{\frac{\rho'}{\rho}}} \tag{A2}$$

where ρ' is a material constant which is determined empirically.

Substituting the value of K_E from equation (A1) into equation (A2) results in the following formula:

$$K_N = 1 + \frac{(K_H - 1)\sqrt{\frac{a}{\rho_e}}}{1 + \sqrt{\frac{\rho'}{\rho_e}}} \tag{A3}$$

L 3 2 8

where ρ_e is used instead of ρ to indicate an effective value of the tip radius for a fatigue crack.

Previous work (ref. 6) indicated that the material constant ρ' was of the same order as the effective radius of a crack ρ_e. As a simplification the two values were assumed to be equal, and equation (A3) becomes

$$K_N = 1 + \frac{1}{2}\left(K_H - 1\right)\sqrt{\frac{a}{\rho_e}} \qquad (A4)$$

REFERENCES

1. McEvily, Arthur J., Jr., and Illg, Walter: The Rate of Fatigue-Crack Propagation in Two Aluminum Alloys. NACA TN 4394, 1958.

2. Illg, Walter: Fatigue Tests on Notched and Unnotched Sheet Specimens of 2024-T3 and 7075-T6 Aluminum Alloys and of SAE 4130 Steel With Special Consideration of the Life Range From 2 to 10,000 Cycles. NACA TN 3866, 1956.

3. Grover, H. J., Hyler, W. S., Kuhn, Paul, Landers, Charles B., and Howell, F. M.: Axial-Load Fatigue Properties of 24S-T and 75S-T Aluminum Alloy as Determined in Several Laboratories. NACA Rep. 1190, 1954. (Supersedes NACA TN 2928.)

4. Head, A. K.: The Growth of Fatigue Cracks. Phil. Mag., ser. 7, vol. 44, no. 356, Sept. 1953, pp. 925-938.

5. Howland, R. C. J.: On the Stresses in the Neighborhood of a Circular Hole in a Strip Under Tension. Phil. Trans. Roy. Soc. (London), ser. A., vol. 229, no. 671, Jan. 6, 1930, pp. 49-86.

6. McEvily, Arthur J., Jr., Illg, Walter, and Hardrath, Herbert F.: Static Strength of Aluminum-Alloy Specimens Containing Fatigue Cracks. NACA TN 3816, 1956.

L 3 2 8

TABLE I.- NUMBER OF CYCLES REQUIRED TO EXTEND FATIGUE CRACKS FROM 0.2 INCH

Stress level, S_o, ksi	Frequency, cpm	Number of cycles to extend crack from 0.2 in. to a length of -											
		0.3 in.	0.4 in.	0.5 in.	0.6 in.	0.8 in.	1.0 in.	1.4 in.	1.8 in.	2.4 in.	3.0 in.	4.0 in.	5.0 in.
2024-T3 aluminum alloy													
[a]2.73	1,800	Crack did not propagate in 10^8 cycles											
[b]3.74	1,800	Specimen failed											
6.00	1,800	275,000	490,000	595,000	560,000	760,000	825,000	898,000	940,000	980,000	1,002,000	1,038,000	1,060,000
10.00	1,800	46,500	66,000	81,000	94,000	113,000	127,500	148,000	162,000	177,000	186,000	193,500	---
20.00	13	3,200	5,370	6,820	7,750	8,970	9,650	10,590	11,250	11,870	12,170	12,440	---
20.00	1,200	3,360	6,210	8,210	9,640	11,260	12,270	13,360	---	---	---	---	---
30.00	9	458	785	1,010	1,150	1,318	1,405	1,506	1,546	1,577	1,592	1,603	---
7075-T6 aluminum alloy													
[c]2.15	1,800	Crack did not propagate in 10^8 cycles											
[b]3.69	1,800	Specimen failed											
6.00	1,800	228,000	357,000	435,000	483,000	540,000	570,000	614,000	645,000	680,000	700,000	---	---
20.0	13	2,970	3,250	6,850	7,900	9,300	10,200	11,330	12,020	12,700	13,100	13,350	---
30.0	9	990	1,550	1,830	2,020	2,250	2,380	2,502	2,558	---	---	---	---

[a]Crack was initiated at S_o = 10 ksi; load was progressively reduced; crack length, 0.73 in.; specimen width, 2 in.

[b]Load was constant throughout test; $K_N S_{net}$ for crack was 26 ksi.

[c]Crack was initiated at S_o = 10 ksi; load was progressively reduced; crack length, 0.66 in.; specimen width, 2 in.

TABLE II.- CALCULATED VALUES OF THE CONSTANT α USED IN INTEGRATION OF RATE EXPRESSION, EQUATION (5)

Crack length, in.	Values of α for stress level, S_o, of -						
	6 ksi	10 ksi	20 ksi	30 ksi	6 ksi	20 ksi	30 ksi
	2024-T3				7075-T6		
0.31	0.0679	1.56	16.8	70.5	0.264	15.7	59.4
.37	.0996	1.63	16.7	71.5	.314	15.3	61.7
.43	.179	1.63	16.3	76.2	.343	14.9	64.1
.49	.161	1.57	16.5	82.4	.365	14.7	67.3
.53	.183	1.70	16.5	85.0	-----	----	----
.55	------	----	----	------	.350	14.5	70.3
.61	.200	1.66	16.6	89.1	.382	14.5	74.2
.67	.215	1.65	16.8	94.1	.384	14.4	80.0
.73	.228	1.64	16.9	99.0	.393	14.6	82.3
.79	.232	1.63	17.1	109	.389	14.8	88.2
.85	.235	1.62	17.3	114	.392	15.2	95.2
.91	.253	1.60	17.9	121	.395	15.6	103
.97	.259	1.63	18.5	132	.395	16.0	112
1.10	.282	1.59	19.6	153	.393	17.0	131
1.60	.315	1.57	23.8	273	.363	20.7	222
2.10	.311	1.60	30.7	502	.342	26.2	396
2.60	.310	1.72	42.2	809	.334	35.2	-----
3.10	.324	1.87	59.6	1458	.343	49.0	-----
3.60	.340	2.12	89.0	2920	-----	75.2	-----
4.10	.375	2.47	14.5	6050	-----	112	-----
4.60	.416	----	----	------	-----	-----	-----
5.00	.481	----	----	------	-----	-----	-----
Weighted average . .	0.150	1.63	17.3	87.1	0.337	15.5	73.9

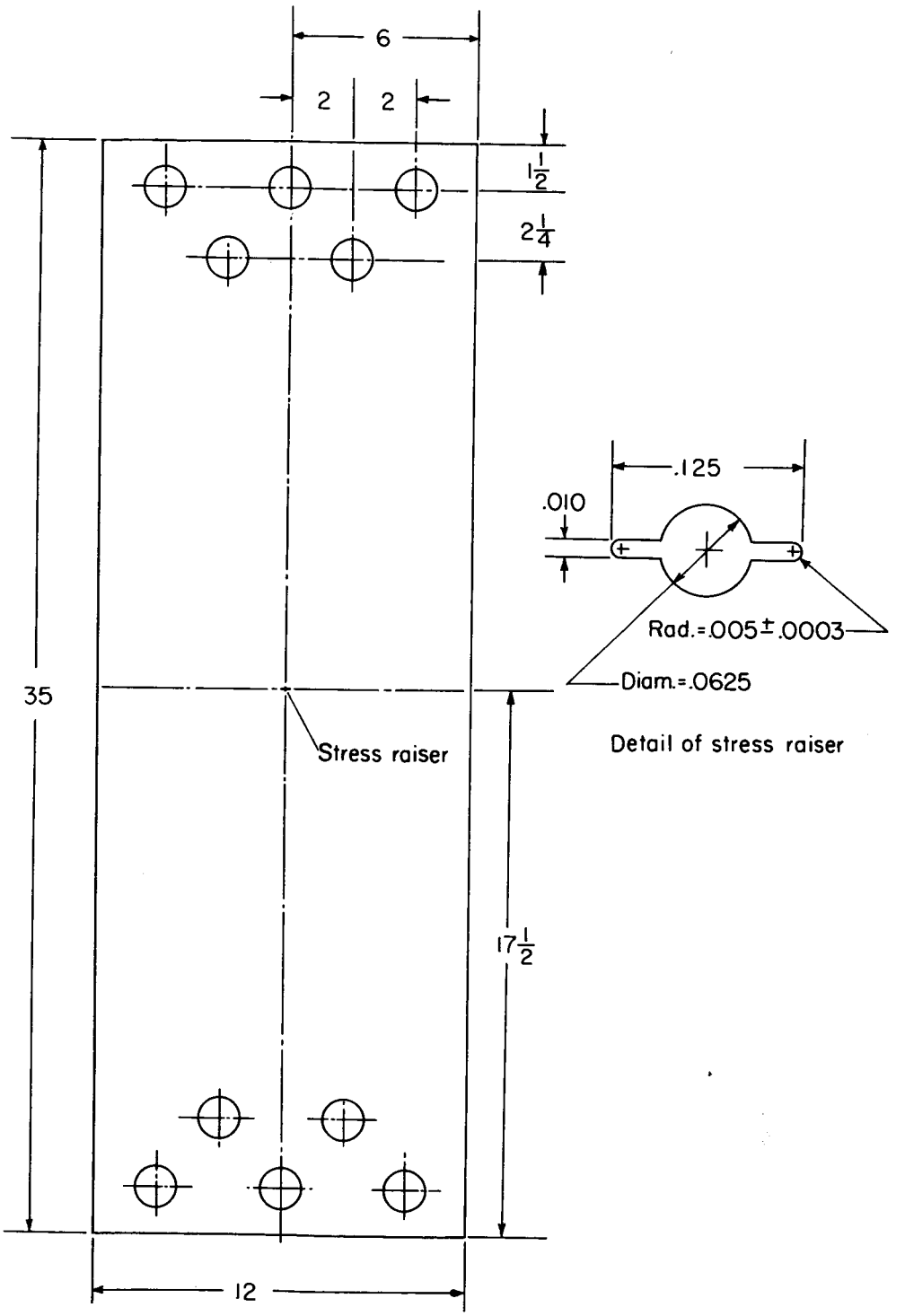

Figure 1.- Configuration of crack propagation specimens.

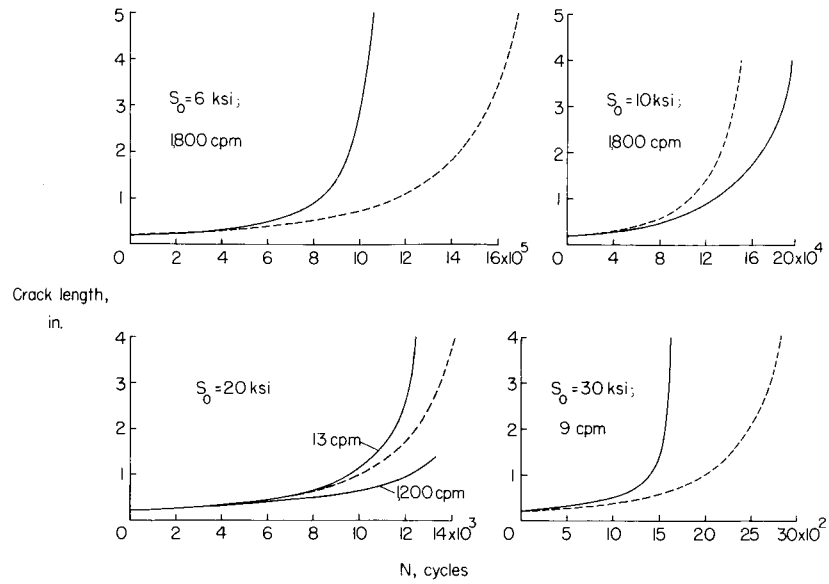

(a) 2024-T3 aluminum alloy.

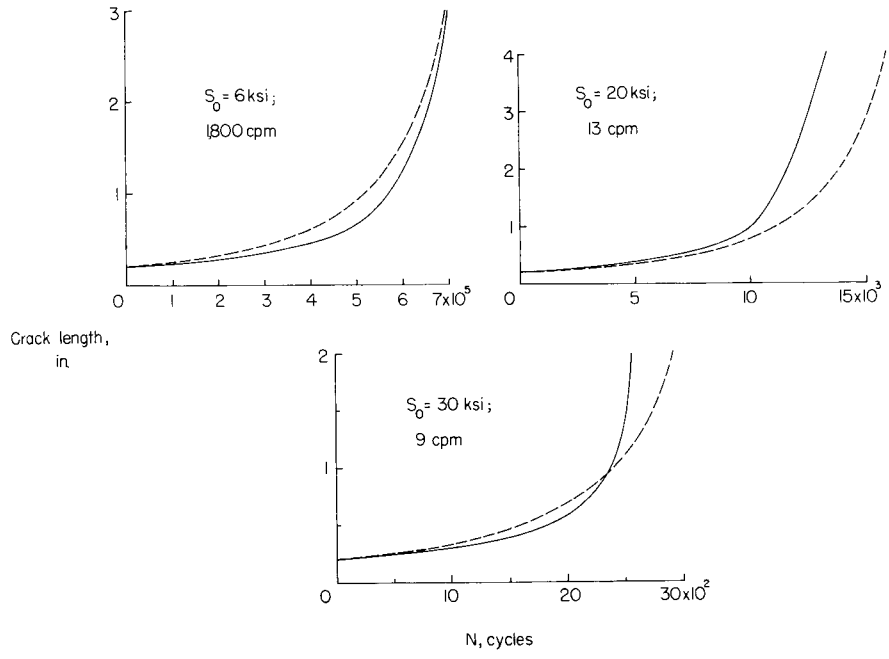

(b) 7075-T6 aluminum alloy.

Figure 2.- Fatigue-crack propagation curves. Solid lines represent experimental results. Dashed lines were computed from $N = C - \frac{1}{\alpha\sqrt{x}}$.

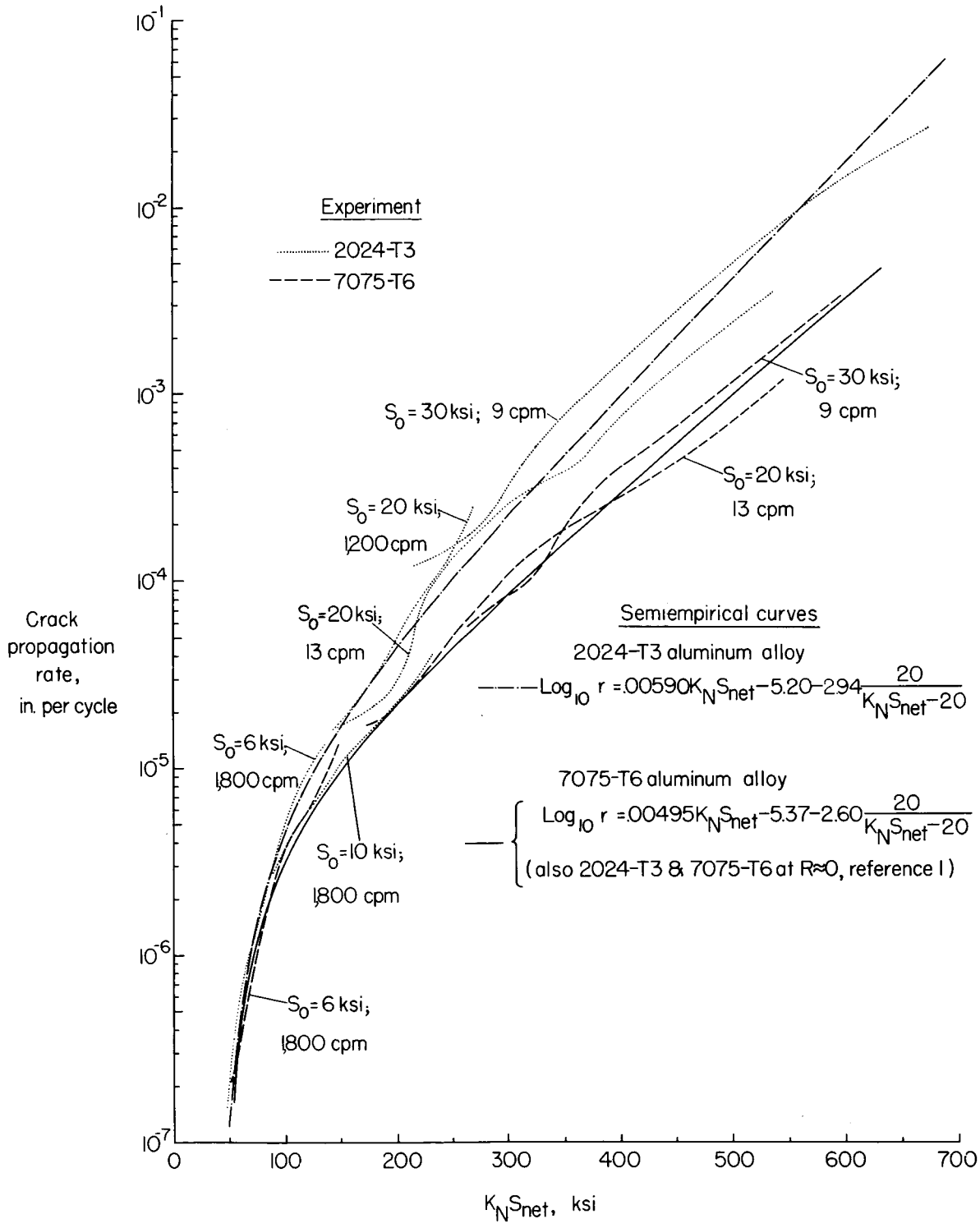

Figure 3.- Rates of fatigue-crack propagation for two aluminum alloys.

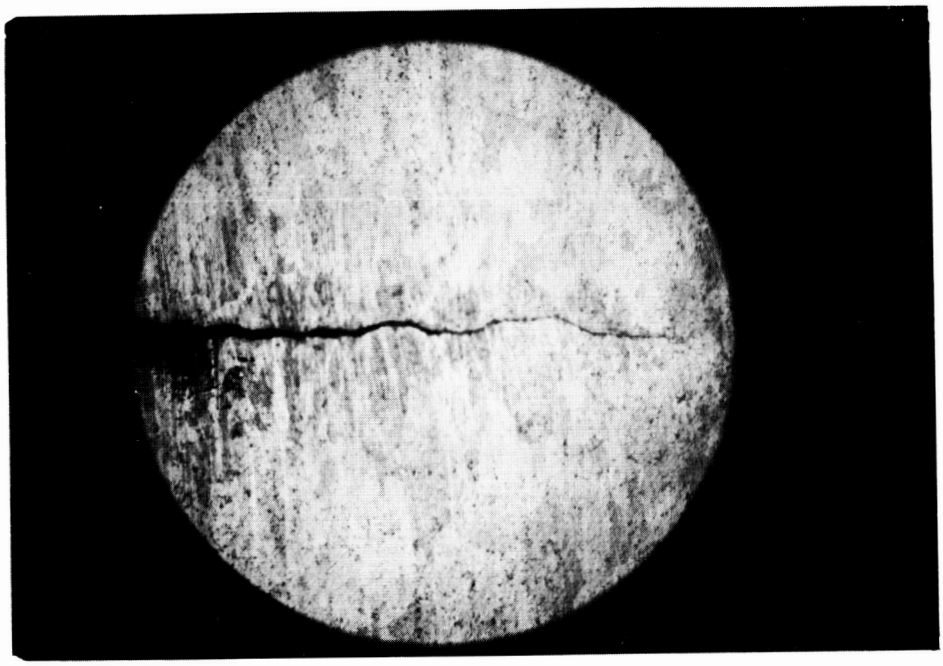

(a) 2024-T3 aluminum alloy.

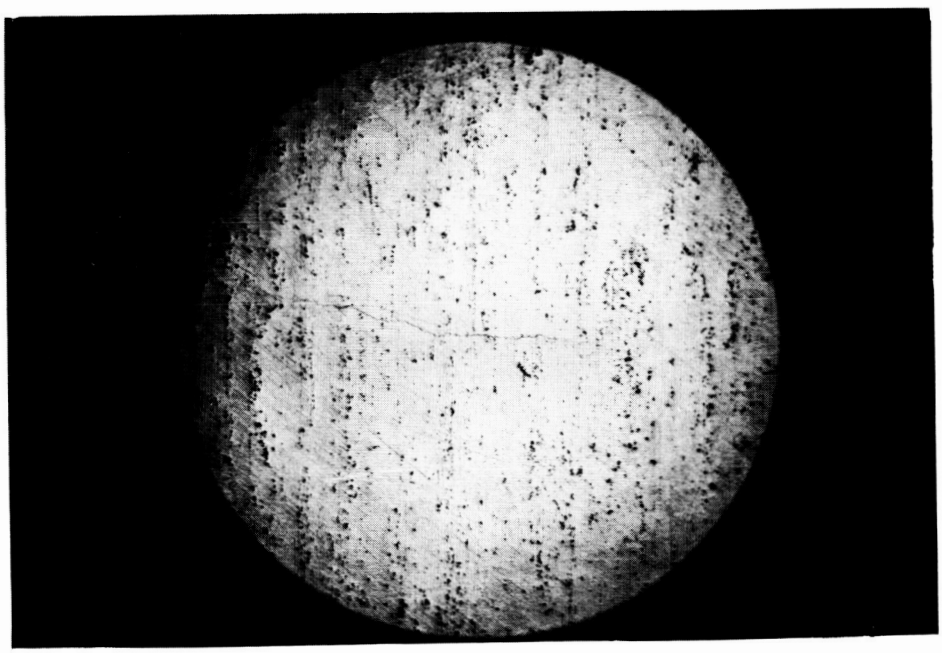

(b) 7075-T6 aluminum alloy. L-59-3088

Figure 4.- Photomicrographs of surface of unloaded sheet specimens. S_o = 30 ksi; x = 1.8 inches. (×25)

L-328

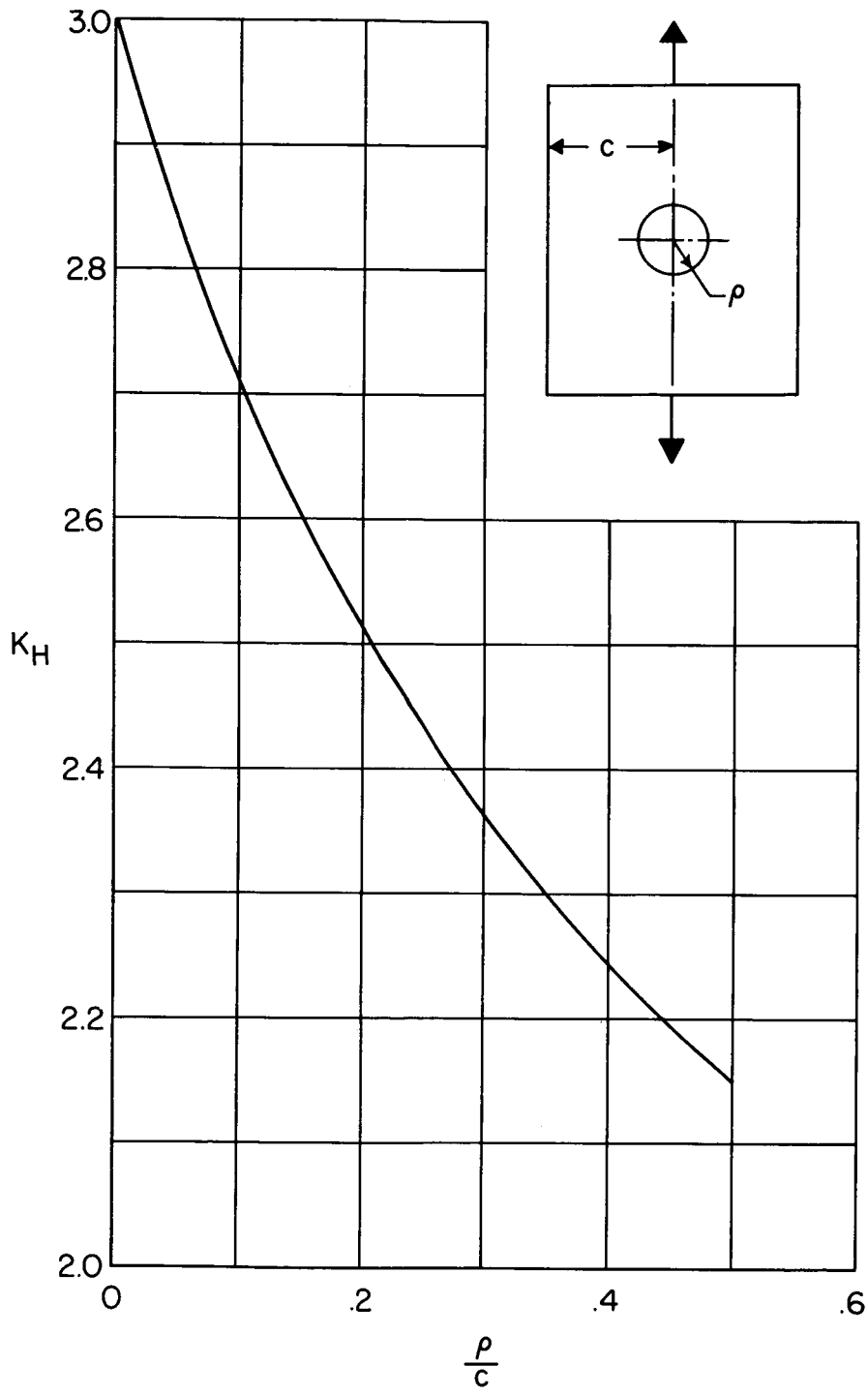

Figure 5.- Elastic stress-concentration factor for a circular hole in a finite sheet (ref. 5).